Electronic Supplementary Material (ESI) for Materials Horizons.

Supporting Information for

Tuning the Reversibility of Hair Artificial Muscles by Disulfide Cross-Linking for Sensors, Switches, and Soft Robotics

*Xueqi Leng, Xiang Zhou, Jiayu Liu, Yicheng Xiao, Jinkun Sun, Yaowang Li, and Zunfeng Liu**

This file includes:

1. Experimental Section

1.1. Characterization of the torsional and the tensile acutation of the hair muscles

The torsional and the tensile actuations of the hair muscle were characterized by recording a video using a fast video camera (Nikon Digital Camera D610), and analysizing the frames from the video. If not specified, the room temperature was 25°C. For the torsional actuation, the hair muscle was vertically suspended and isobarically loaded with a rectanglular paddle (2.5 mm × 0.5 mm × 0.1 mm) with the mass of 0.013 g. For the actuation, the muscle fiber that was in the open enviromental air with the humidty of 20% was transferred into a vessle with high humidity and started rotating. After the rotation stopped, it was put back into the enviromental air. Alternatively, the torsional hair muscle was actuated by exposing to the ultra-sonically generated water fog in the open air. The rotation angle and the rotational speed were obtained by counting the frames in the video.

For the tensile actuation, the hair coil after chemical shape fixing was vertically suspended free of load and without torsional tethering. Initially the hair coil was put in the open enviromental air with the humidty of 20%, then it was transferred into a vessle with high humidity and started contracting or elongating. After the hair muscle stopped actuating, it was put back into the open enviromental air. Alternatively, the tensile hair muscle was actuated by being esposed to the ultra-sonification generated water fog in the open air. The tensile actuation stroke and the speed were obtained by counting the frames in the video.

1.2 Equipments used for characterization of hair fibers

The measurement of the mechanical properties of the hair fibers were carried out on the mechanical test machine modeled HENGYI 0580 equipped with a 5 N load cell. The gauge lenth was 20.0 mm, and the extension rate was 10.0 mm min^{-1}. The optical images of the hair fibers were obtained on a OLYMPUS microscope (model CX31). The SEM of hair fibers was carried out on a FEI Quanta microscope (QUANTA 200). FTIR spectroscopy of the hair fibers was carried out on a TENSOR 37 FTIR spectrometer. Raman spectroscopy of the hair fibers was carried out on a high resolution micro Raman spectrometer (LABRAM HR EVO). The X-ray diffraction patterns were obtained on an Ultima IV X-ray diffractometer (Cu Kα radiation), and the scanning diffraction angle was from 5° to 40°. A Rigaku X-ray diffractometer (BioSAXS-2000, MicroMax 007 HF) was also used to obtain the two dimensional X-ray diffraction patterns of the hair fibers. The ambient temperature and the relative humidity were obtained on a hygrometer (CEM DT-615).

1.3. Mechanism of the reversible and irrversible hair fiber artificial muscles

Based on the microstructural evolution of the hair fiber actuators during the twist insertion, the chemical cross-linking, and the actuation, we proposed a possible mechanism for the twist-containing hair fiber actuator with the tunable reversible and irrversible actuations. In order to obtain the tether-free reversible hair muscle, we first need to adequately cleave the pristine S-S bond to form the –SH bonds, by chemical reduction reaction using the ammonium thioglycollate solution. Subsequently, adequate oxidation reaction of the above hair fibers by using the lauramine oxide solution to re-form the new S-S bond. In this way, the inserted twist can be preserved by formation of the new S-S cross-linking network of the hair artificial muscle (Figure 2D (i)). During the hygromorph actuatiton, the newly formed S-S cross-linking network was not destroyed, and the inserted twist was preserved during the repeated actutaiton cycles. This is the reversible hair artificial muscle. If this oxidation reaction is not adequate enough to produce enough S-S cross-linking points, the cross-linking network can not be preserved during the hygromorph actuation of the hair fiber. As a result the preserved twist was released after one cycle of the actuaiton. This is the irreversible hair artificial muscle (Figure 2D(ii)).

1.4. Testing processes on the diameter variation of the hair on the humidity adsorption

The changes in the diameter and the length were measured on an optical microscope by exposing a short segment of the hair fiber (5 cm) to the ultrasonically generated water fog (0.22 g s^{-1} m^{-2}). Images were taken before and 1 min after water exposure to the hair fiber to ensure fully water absorption (Fig. 2G). The diameter and the length were measured from the pictures. The volume can be calculated using the following equation: $V = \pi(d/2)^2 l$, where V is the volume of the hair fiber, d is the diameter of the hair fiber, and l is the length of the hair fiber.

1.5. Applications of the hair fiber artificial muscles

The large tensile stroke of the hygromorph hair coil allowed us to prepare an optically readable moisture sensor. Ten plies of the twisted hair fibers were folded in the middle point, then wrapped around a mandrel to form a homochiral coil, and they were soaked in the ammonium thioglycollate solution (600 mM) for 15 min for the chemical reduction, followed by soaking in the lauramine oxide solution (130 mM) for 10 min for the chemical oxidation. The spring index was 2.78, the coil pitch was 3 mm, the twist density was 1000 turns m^{-1}, and the ambient humidity was ~20%. The shape of the hair coil was stabilized after removing the mandrel, and the fiber artificial muscle showed reversible hygromorph actuation behavior. Such a homochiral hair fiber artificial muscle can be directly used as an optically readable moisture sensor, because it exhibited monotonically decreasing length when it is equilibrated in different-humidity environment (Fig. 5D, Fig. S27 and Movie. S1). A homochiral hair coil was also used as a hygromorph electrical switch for a smart alarm. In the dry air (20%), the light emitting diodes (LEDs) were connected to the electrical supply by the copper plate loaded at the end of the hair coil fiber artificial muscle and lightened; when the hair coil was exposed to the water fog, the electric circuit was disconnected, and the LEDs went out (Fig. 5E,F and Movie. S2). As another example, two independently actuated heterochiral coil artificial muscles can be assembled in parallel to control the forward moving of a soft robot (Fig. 5H and Movie S10).

Changing of styles of the hair or the feather has been used as the smart response by the animals or the birds to communicate with others or protect themselves against the predators. For example, when the squirrels saw something dangerous, they alerted other squirrels by wagging their tails; the peacocks attracted the attention of the peahens by fanning out their tail feathers to show the pretty eye spots, and shaken these feathers when they wanted to mate; the hedgehogs made their spines immediately brittle up when they felt threatened. Since 1870s people have marcelled their hair to a wave style by using the hot curling tongs, and later on the disulfide cross-linking (the cold marcelling technique) was developed to make the coiled or the flattened hairs by treating the hair with the reducing reagent followed by using the oxidant. Up till now, the marcelling techniques were not able to produce hair styles that can reversibly change the shape in response to the environmental changes.

Here we developed a smart hair style that can reversibly respond to humidity by this twist-assisted disulfide cross-linking, which was realized by twist insertion into hair fibers followed by reduction and oxidation. Then hair fiber artificial muscle prepared in a similar way as the previous paragraph (without folding in the middle after twist insertion) were attached on the head of a doll in parallel to form a moisture-sensitive smart hair style. In detail, ten plies of 20-cm-long, 95-μm-diameter adult female hair fibers were twisted until just before coiling (2000 turns m^{-1}) at an isobaric load of 2.1 MPa. Then it was wrapped around a 3-mm-diameter mandrel to form a homochiral coil with the spring index of 3.4 and the coil pitch of 3 mm. Then the hair coil on the mandrel was both end tethered and soaked in the ammonium thioglycollate solution (600 mM) for 15 min for reduction, followed by soaking in the lauramine oxide solution (130 mM) for 10 min for oxidation to obtain the reversible hygromorph artificial muscle. By spraying the water droplets on the hair coils, they shrank by ~80% in 2.5 min, and upon water evaporation into air they returned back to the initial length (Fig. 5G, Movie. S3). Such a smart hair style may be used in the environmental adaptive cases that got short to facilitate sweat evaporation from the body.

1.6. Calculation of the extent of the reformed S-S bond by oxidation of the chemically reduced –SH bond.

Figure S2 shows the Raman spectra of the hair for the different chemical reduction time. The peak at 580 cm^{-1} for the untreated hair fiber corresponded to the S-S bond, and this peak red shifted and the intensity decreased due to the breakage of the S-S bond to form the –SH bond during the chemical reduction; oxidation of the chemically reduced hair fiber resulted in the reversible blue shift of this peak. Because oxidation of the pristine hair fiber did not cause noticeable change of this peak (data not shown), we considered the S-S bond that was able to be chemically reduced to be 100%. We then quantitatively calculated the percentage of the reformed S-S bond by dividing the increase for the integrated area for the peak between 500 and 600 cm^{-1} during further oxidation of the hair fiber with the reduction time of 15 min. Figure S3A shows the dependence of the percentage of the reformed S-S bond as a function of the oxidation time for the chemically reduced hair fiber. The hair fiber with the oxidation time of 2 and 10 min showed the fully irreversible and the fully reversible actuations, respectively (Fig. S3B).

1.7. Discription of the Equations 2 to 4.

The torsional rotation angle can be calculated from the inserted twist and the change in fiber diameter, which was derived from the reference 20 (*Science* 2014, 343, 6173) and our previous work (*Adv. Funct. Mater*., 2019, 29, 1808241). We have added this information into the revised manuscript, and give brief introduction of the equations 2 to 4. The detailed information about these equations from the reference 20 is shown below.

The description of the equation 2 is as follows (from *Science* 2014, 343, 6173): "For a twisted fiber until just before coiling, initially parallel fiber is twisted into helices that have a bias angle (α) relative to the fiber direction of approximately $\alpha = \tan^{-1}(2\pi r T)$, where r is the radial distance from the fiber center and T is the amount of twist inserted per initial fiber length.[1] The cross-section of pristine hair fiber is approximated to a circle, and the diameter is twice the radius (d=2r), so the equation can be summed up as $\alpha = \tan^{-1}(\pi d_e T)$."

For the equation 3, because of the hair fiber could get flattened during twist insertion, the original diameter is not suitable for the twisted hair fiber. But the area of the cross-section would not change before and after twist insertion, so we use this condition to build an equation to get the equivalent fiber diameter (d_e). This equivalent fiber diameter was approximated from the following equation: $\pi(d_e/2)^2 = d_s d_l$, where d_s and d_l were the lengths of the short side and the long side across the cross-section of the flattened hair fiber, respectively, by roughly approximating the cross-section of the flattened hair was rectangular.

The equations 4 was derived from the reference 2 (*Adv. Funct. Mater., 2019, 29(18), 1808241*). When applied to a twisted hair fiber, this model predicts that the relative change in the inserted twist is given by $\frac{\Delta n}{n} = \frac{\frac{\Delta\lambda}{\lambda}}{cos^2\alpha_f} - \frac{\Delta d}{d} - (\Delta l/l)tan^2\alpha_f$, where n is the inserted twist, λ is the length of a helical fiber in the twisted fiber, d is the initial diameter of the twisted fiber before actuation, l is the axial length of the twisted fiber, and Δ indicates changes in these parameters during actuation. According to above Equation, expansion in the fiber diameter due to absorption of water leads to torsional actuation by yarn untwist. For this hair artificial muscle, $\Delta\lambda/\lambda$ and $\Delta l/l$ are relatively small because of the high fiber modulus in their axial directions. The torsional actuation is thus approximated as $\Delta T = -T(\Delta d_e/d_e)$, where T is the initially inserted twist n when normalized to initial fiber length before twist insertion and ΔT is the change in T during actuation, d_e was the equivalent fiber diameter as the hair got flattened during twist insertion.

2. Supplementary Figures

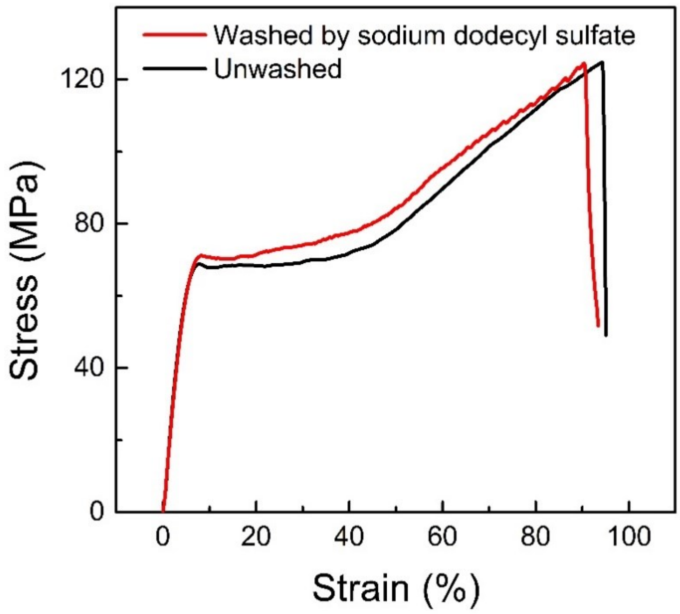

Figure S1. Stress-strain curves for an as obtained human hair fiber and the hair fiber after washing with the sodium dodecyl sulfate solution (0.5 wt%) and air dried. The relative humidity of ambient air was ~20%. Negligible change in the mechanical properties was observed for the hair fibers before and after washing.

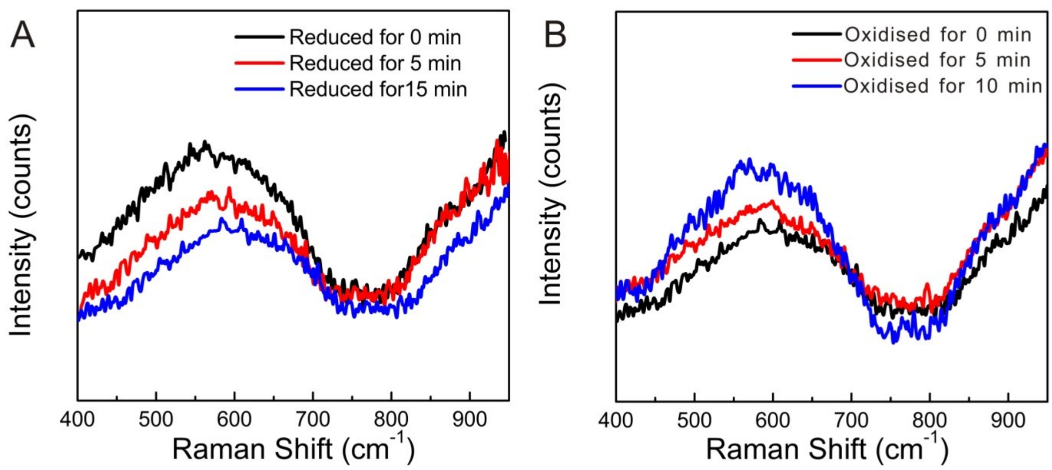

Figure S2. Raman spectra of the hair fibers by soaking the hair fiber in the ammonium thioglycollate solution (600 mM) for different time for the chemical reduction (A), and for the hair fibers with 15 min reduction time that were further soaked in the lauramine oxide solution (130 mM) for different oxidation time (B).

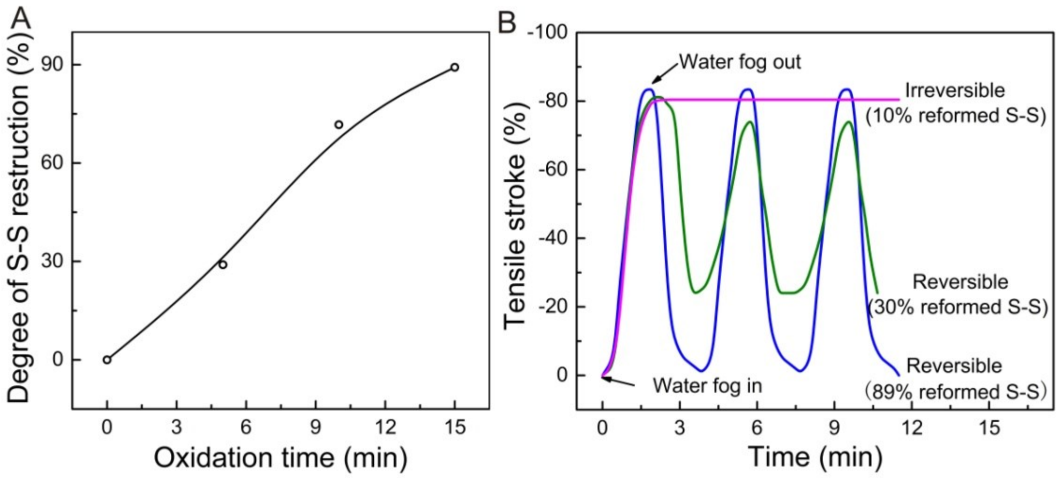

Figure S3. Degree of the S-S reconstruction for the hair fibers with the 15 min reduction time that were further soaked in the lauramine oxide solution (130 mM) for different oxidation time (A). Tensile stroke as a function of time for the typical irreversible actuation, the reversible actuation with lower degree of the S-S reconstruction (30%) and the reversible actuation with high degree of the S-S reconstruction tensile hair artificial muscles (89%) (B).

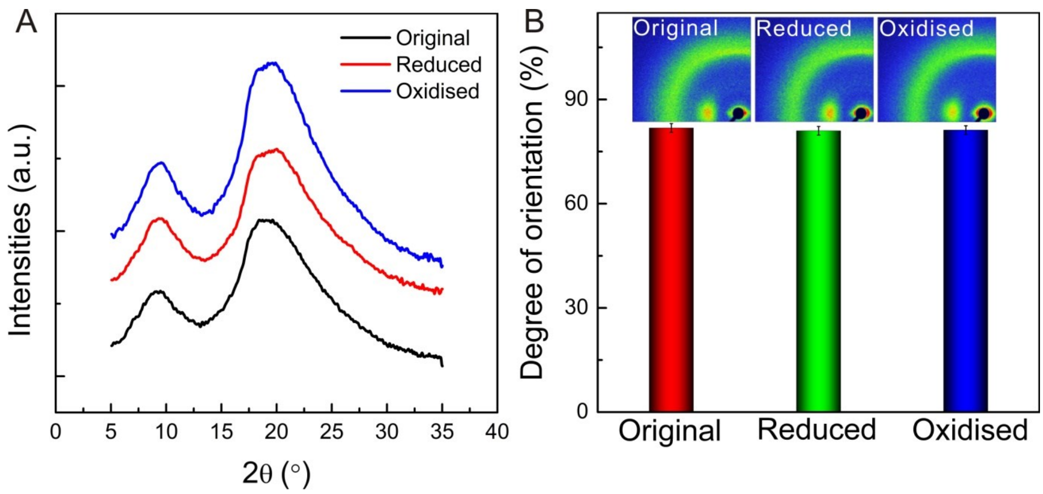

Figure S4. The integrated intensity curves (A) and the degree of orientation of the 2D WAXS X-Ray diffraction patterns (B) for the original hair fiber, the hair fiber after the chemical reduction, and this fiber after the chemical oxidation. The hair fiber was soaked in the ammonium thioglycollate solution (600 mM) for 15 min for chemical reduction, and this hair fiber was soaked in the lauramine oxide solution (130 mM) for 10 min for chemical oxidation.

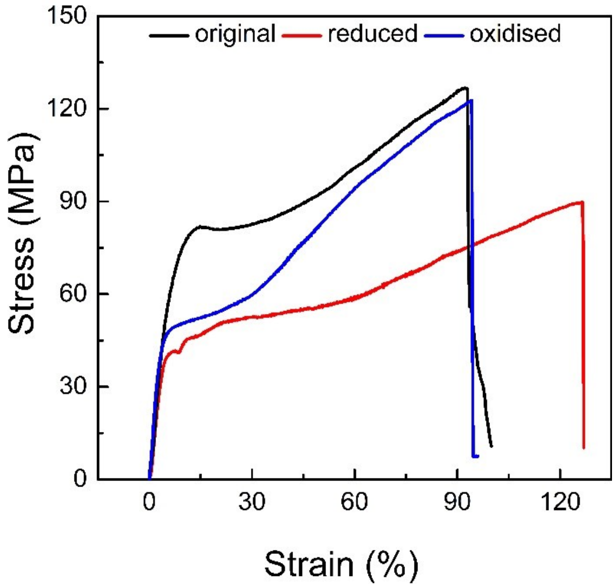

Figure S5. Stress-strain curves for the pristine hair fiber, the hair fiber after chemical reduction, and this fiber after chemical oxidation. The hair fiber was soaked in the ammonium thioglycollate solution (600 mM) for 15 min for chemical reduction, and this hair fiber was soaked in the lauramine oxide solution (130 mM) for 10 min for chemical oxidation.

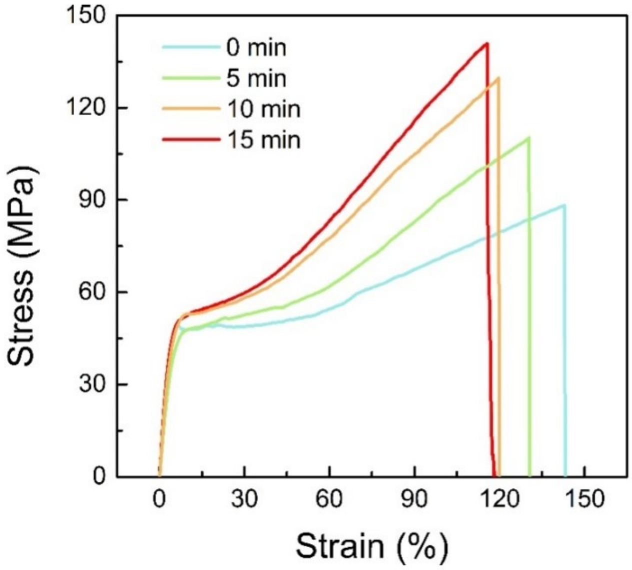

Figure S6. Stress-strain curves of the human hair fiber that was soaked in the ammonium thioglycollate solution (600 mM) for 20 min for chemical reduction, followed by soaking in the lauramine oxide solution (130 mM) for different time for chemical oxidation. The relative humidity of ambient air was ~20%.

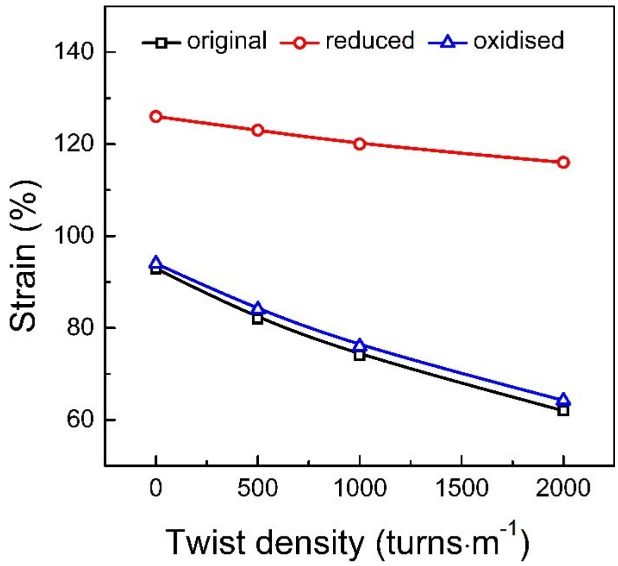

Figure S7. Mechanical properties of the hair fibers treated with the chemical reduction, the chemical oxidation, and the twist insertion. Strain at break as a function of the twist density for the pristine hair fiber, the hair fiber after the chemical reduction, and the fiber after sequential chemical reduction and oxidation. For chemical reduction the hair fiber was soaked in the ammonium thioglycollate solution (600 mM) and for chemical oxidation the hair fiber was soaked in the lauramine oxide solution (130 mM). The ambient humidity was 20%, and the strain rate was 0.83% s^{-1}.

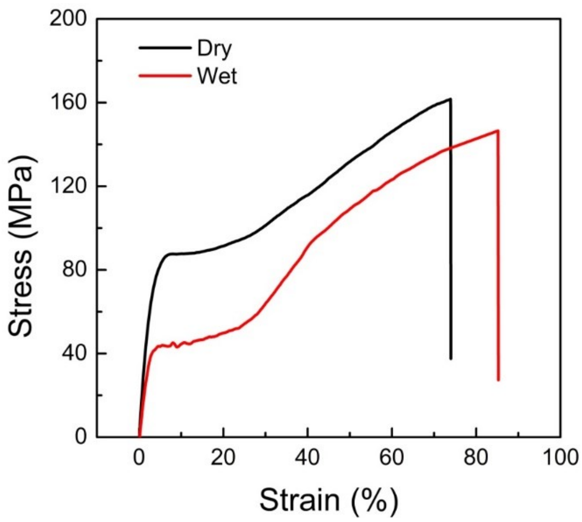

Figure S8. Stress-strain curves for the pristine dried hair fiber and this hair fiber that was soaked in water for 1 min. The ambient humidity was 20%, and strain rate was 0.83% s^{-1}.

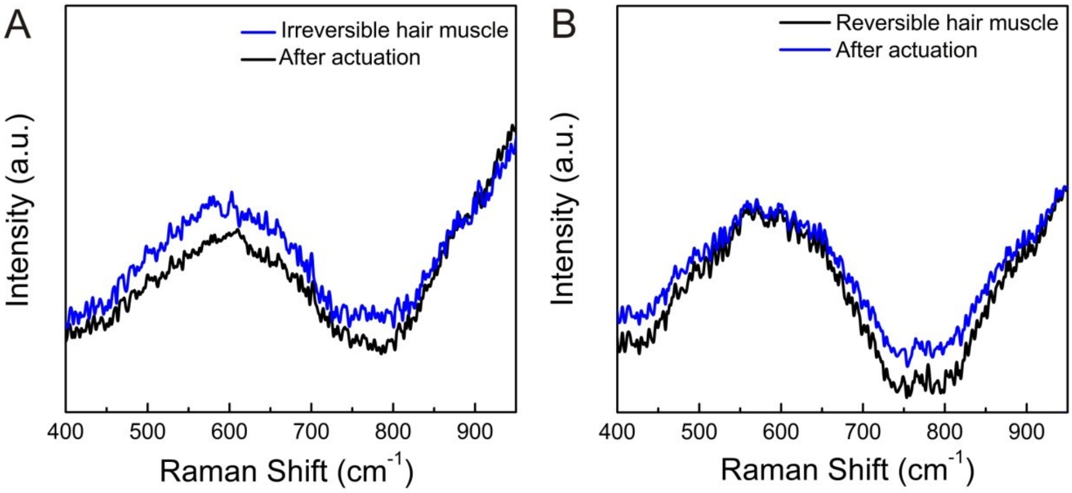

Figure S9. Raman spectra of the torsional hair muscles with (A) the irreversible and (B) the reversible actuation before and after the moisture-driven actuation on exposure to the water fog. For (A) the muscle was prepared by soaking the twisted human hair (1500 turns m^{-1}) in the ammonium thioglycollate solution (600 mM) for 15 min for chemical reduction, and further soaked in the lauramine oxide solution (130 mM) for 2 min for chemical oxidation. The ambient air humidity was 20%. For (B) the muscle was prepared by soaking the twisted human hair (1500 turns m^{-1}) in the ammonium thioglycollate solution (600 mM) for 15 min for chemical reduction, and further soaked in the lauramine oxide solution (130 mM) for 10 min for chemical oxidation.

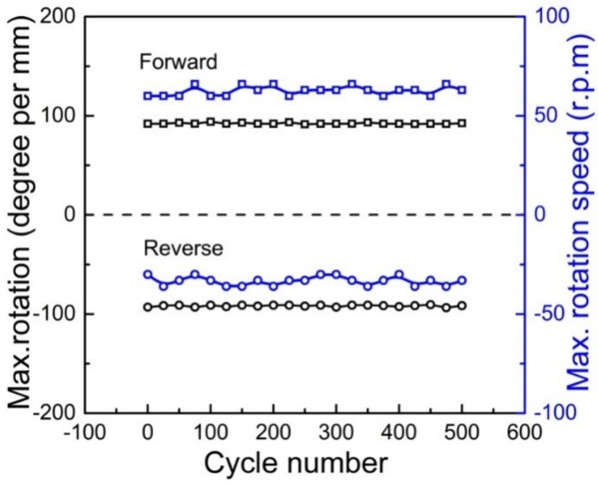

Figure S10. The maximum rotation angle and the maximum rotational speed as a function of the actuation cycles for the reversible hair muscle on exposure to the water fog. The hair muscle were soaked in the ammonium thioglycollate solution (600 mM) for 15 min for reduction, followed by soaking in the lauramine oxide solution (130 mM) for 10 min for oxidation to produce reversible muscle; the twist density was 1500 turns m^{-1}.

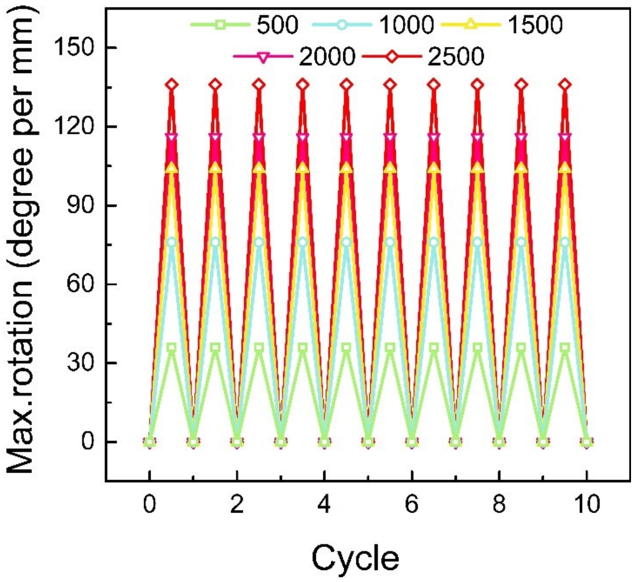

Figure S11. The maximum rotation angle for tens cycles of actuation for the torsional hair muscle with different twist density on exposure to the water fog. The torsional hair muscle was prepared by soaking the twisted hair fiber in the ammonium thioglycollate solution (600 mM) for 15 min for chemical reduction, followed by chemical oxidation in the lauramine oxide solution (130 mM) for 10 min, to give a reversible torsional muscle. The unit of the twist density in the figure was turns m^{-1}. The ambient humidity was 20%, and the flux of the water fog was 0.22 g s^{-1} m^{-1}.

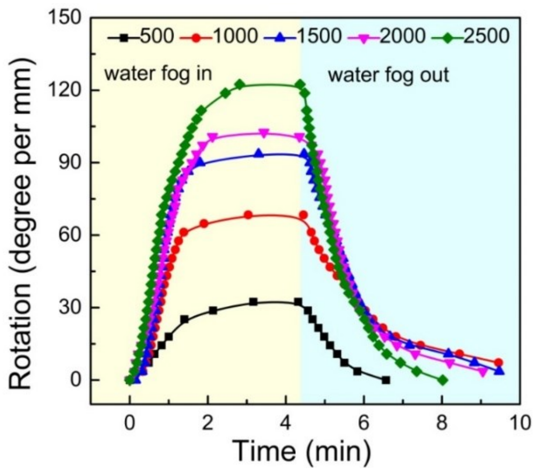

Figure S12. Rotation angle as a function of time for the torsional hair muscle with different twist density during exposure to the water fog and removal of the water fog. The torsional hair muscle was prepared by soaking the twisted hair fiber in the ammonium thioglycollate solution (600 mM) for 15 min for chemical reduction, followed chemical oxidation in the lauramine oxide solution (130 mM) for 10 min, to give a reversible torsional muscle. The unit of the twist density in the figure was turns m^{-1}. During actuation, the ambient humidity was 20%, and the flux of the water fog was 0.22 g s^{-1} m^{-1}.

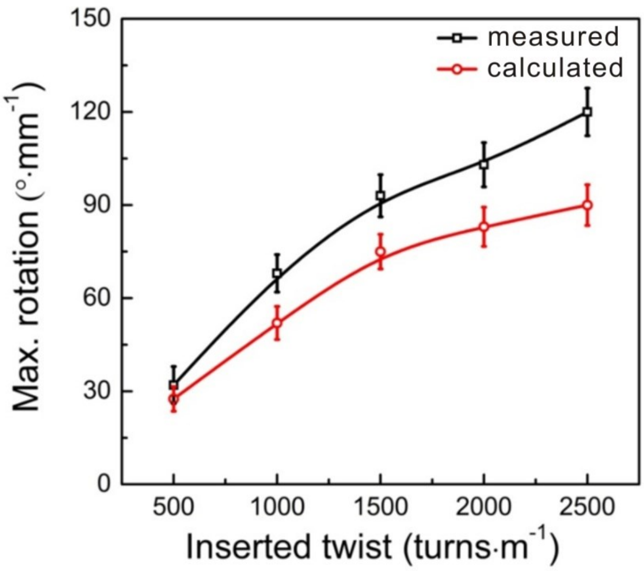

Figure S13. The experimentally measured and the theoretically calculated maximum rotation angles as a function of the inserted twist for the torsional hair muscle on exposure to the water fog. The torsional hair muscle was prepared by soaking the twisted hair fiber in the ammonium thioglycollate solution for 15 min for chemical reduction, followed by chemical oxidation in the lauramine oxide solution for 10 min, to give a reversible torsional muscle. During actuation, the ambient humidity was 20%, and the flux of the water fog was 0.22 g s^{-1} m^{-1}.

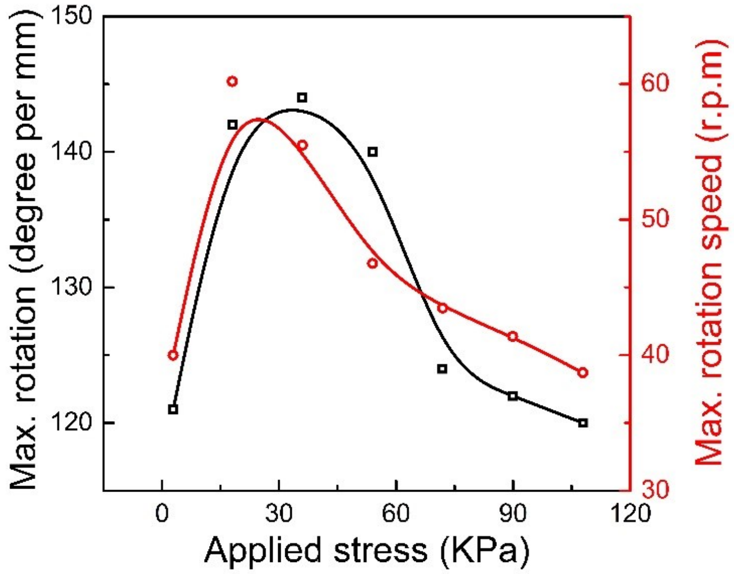

Figure S14. The maximum rotation angle and the maximum rotational speed as a function of the applied stress for the torsional hair muscle on exposure to the water fog. The torsional hair muscle was prepared by soaking the twisted hair fiber in the ammonium thioglycollate solution for 15 min for chemical reduction, followed by chemical oxidation in the lauramine oxide solution for 10 min, to give a reversible torsional muscle. During actuation, the ambient humidity was 20%, and the flux of water fog was 0.22 g s^{-1} m^{-1}.

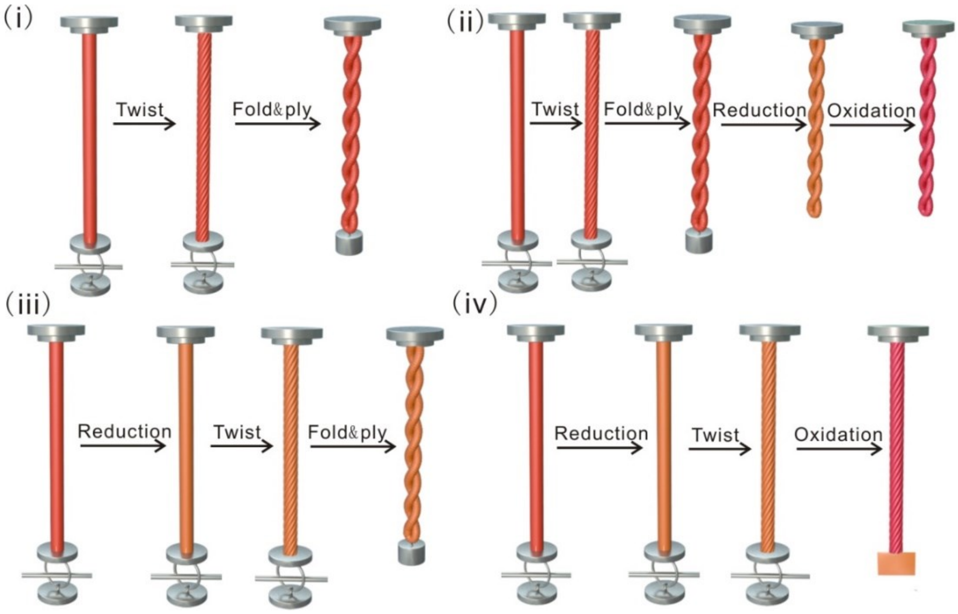

Figure S15. Schematic illustration of the different ways to prepare the torsional hair muscle. (i) Twist insertion into the hair fiber, followed by folding the fiber in the middle point to form a two-ply structure (abbreviated as twisted and two ply); (ii) Folding the twisted hair fiber in the middle point to form a two-ply structure, chemical reduction in the ammonium thioglycollate solution, and oxidation in the lauramine oxide solution (abbreviated as twisted, two ply, reduced and oxidized); (iii) Chemical reduction of the hair fiber in the ammonium thioglycollate solution, followed by twist insertion and folding in the middle point to form a two-ply structure (abbreviated as reduced, twisted, and two ply); (iv) Chemical reduction of the hair fiber in the ammonium thioglycollate solution, followed by twist insertion, and chemical oxidation of the hair fiber in the lauramine oxide solution (abbreviated as reduced, twisted, and oxidized).

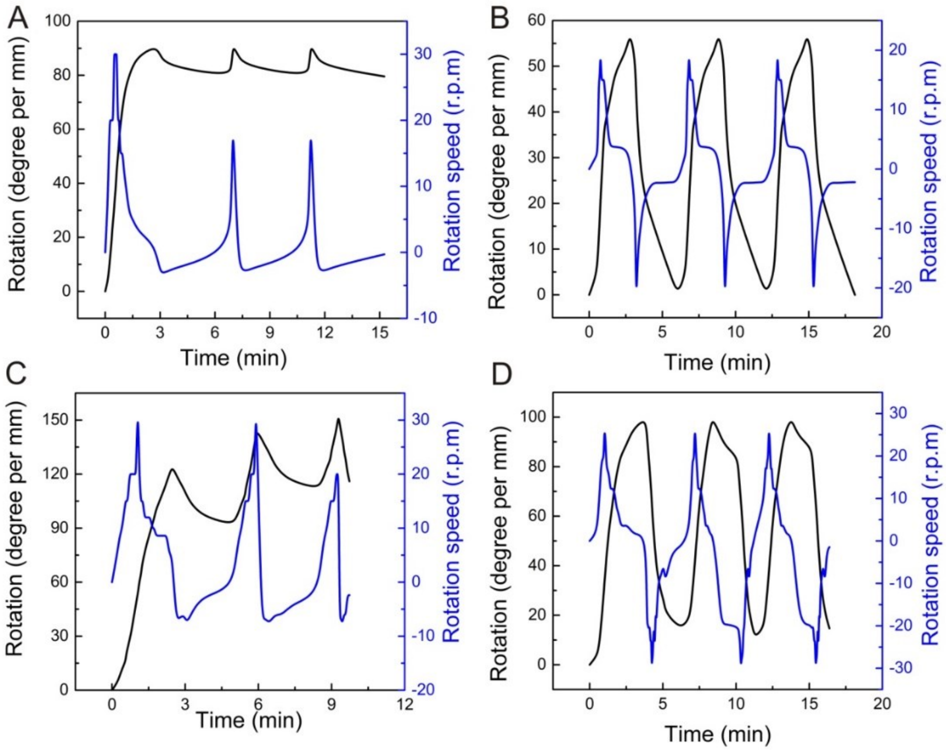

Figure S16. The rotation angle and the rotational speed on exposure to the water fog for the torsional hair muscles prepared by different methods in Fig. S17. (**A**) Twisted and two ply. (**B**) Twisted, two ply, reduced and oxided. (**C**) Reduced, twisted, and two ply. (**D**) Reduced, twisted, and oxidaed. For (A) to (D), the twist density was 1500 turns m^{-1}, the chemical reduction was done by soaking the hair fiber in the ammonium thioglycollate solution (600 mM) for 15 min, and the chemical oxidation was done by soaking the hair fiber in the lauramine oxide solution (130 mM) for 10 min. The ambient humidty was 20%, and the flux of the water fog was 0.22 g s^{-1} m^{-1}.

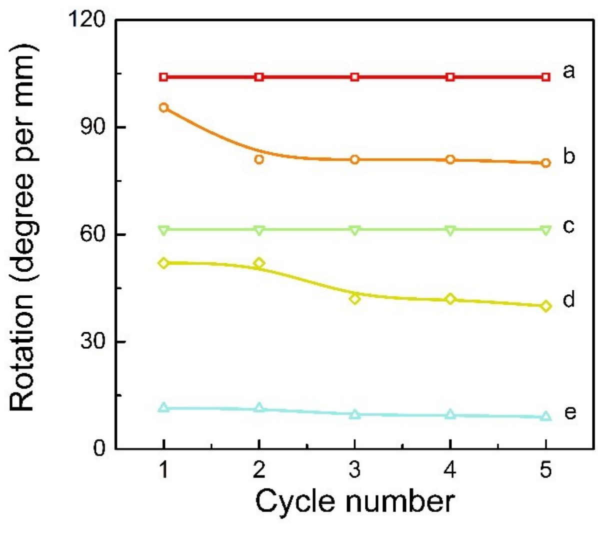

Figure S17. The rotation angle on exposure to the water fog for the torsional hair muscles prepared by different methods: (a) Twisted, reduced, and oxided; (b) Reduced, twisted, and oxided; (c) Twisted, two ply, reduced and oxided; (d) Reduced, twisted, and two ply; (e) Twisted and two ply.

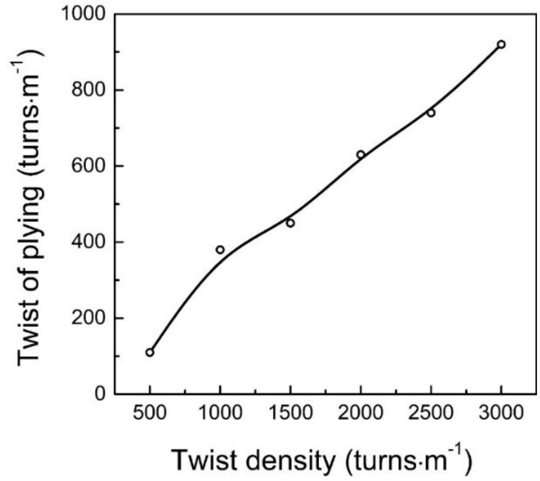

Figure S18. Twist of plying as a function of the twist density of the hair fiber, where the twisted fiber was folded in the middle point to form a two-ply structure.

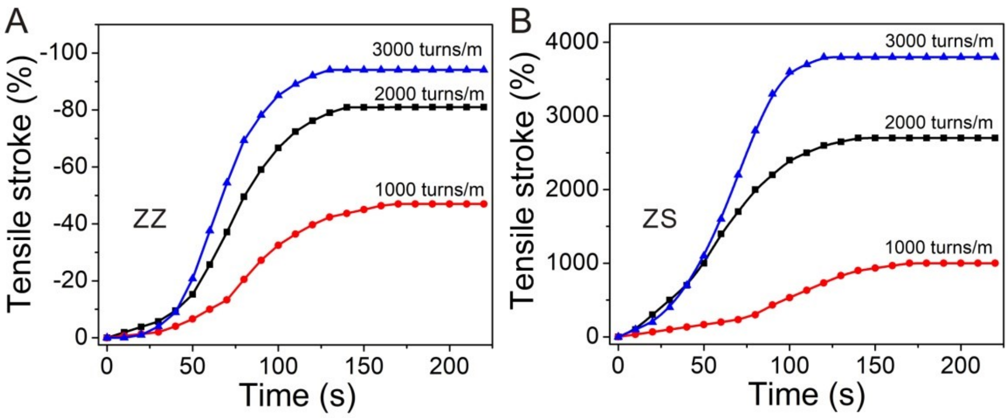

Figure S19. Tensile stroke as a function of time for (A) the homochiral and (B) the heterochiral hair coils with different inserted twist on exposure to the water fog. For (A) and (B), the hair coils were soaked in the ammonium thioglycollate solution (600 mM) for 15 min for reduction, followed by soaking in the lauramine oxide solution (130 mM) for 10 min for oxidation; the pitch for the homochiral coil was 3 mm, and the coils contacted with each other for the heterochiral coil. The spring index for (A) and (B) was 15.8. The flux of water fog was 0.22 g s^{-1} m^{-1}.

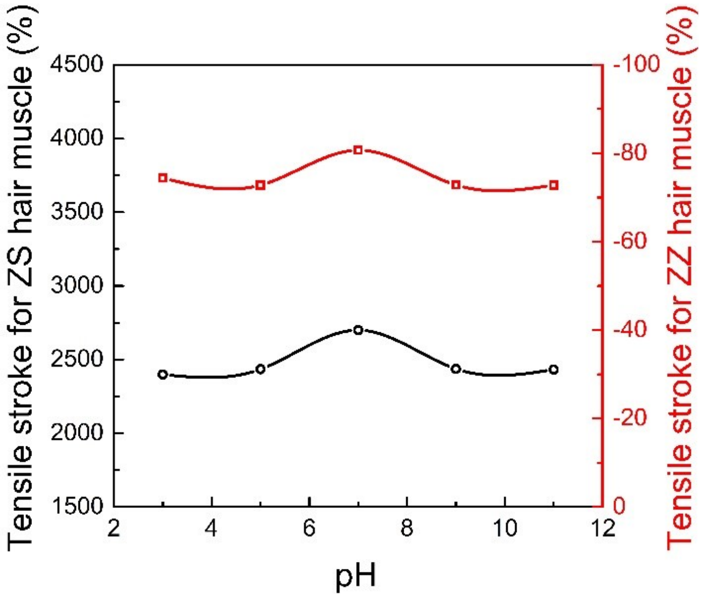

Figure S20. Tensile stroke for the homochiral and the heterochiral hair coils on exposure to the water fog with different pH values. The hair coil was soaked in the ammonium thioglycollate solution (600 mM) for 15 min for reduction, followed by soaking in the lauramine oxide solution (130 mM) for 10 min for oxidation; the twist density was 2000 turns m^{-1}, the spring index was 15.8, the coil pitch for the homochiral coil was 3 mm and the coils contacted each other for the heterochiral coils, and the flux of the water fog was 0.22 g s^{-1} m^{-1}.

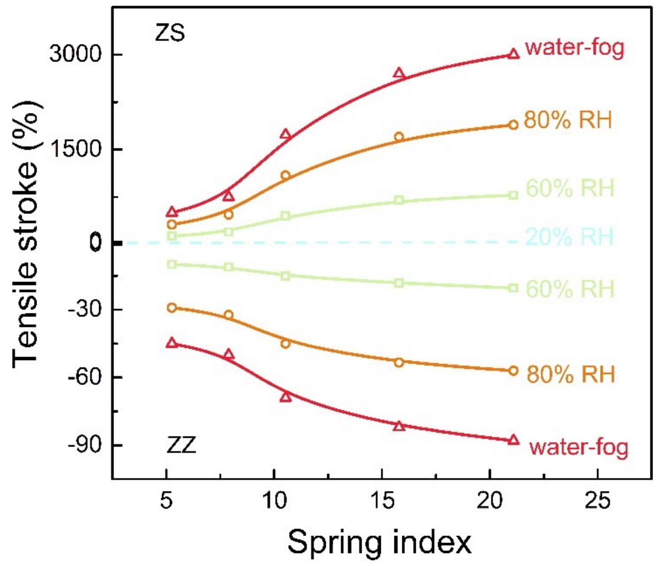

Figure S21. Tensile stroke as a function of the spring index for the homochiral and the heterochiral hair coils on exposure to different humidity air and the water fog.

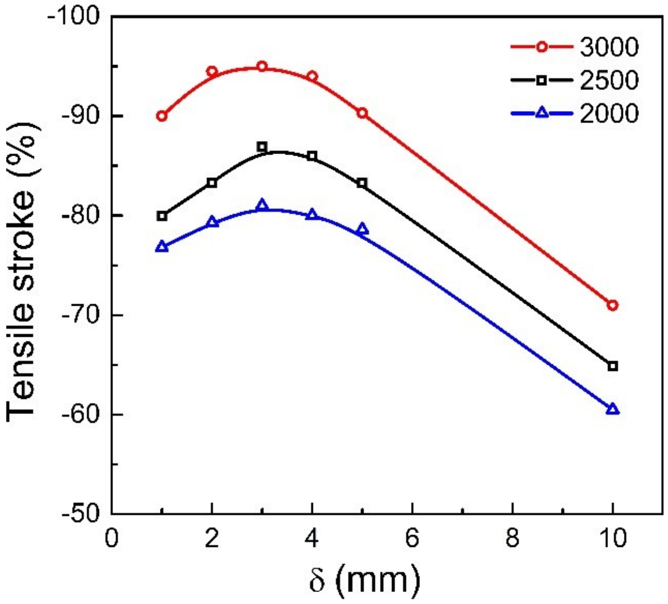

Figure S22. Tensile stroke as a function of the coil pitch for the homochiral hair coils with different twist density on exposure to the water fog. The hair coils were soaked in the ammonium thioglycollate solution (600 mM) for 15 min for reduction, followed by soaking in the lauramine oxide solution (130 mM) for 10 min for oxidation; the spring index was 15.8, and the flux of the water fog was 0.22 g s^{-1} m^{-1}.

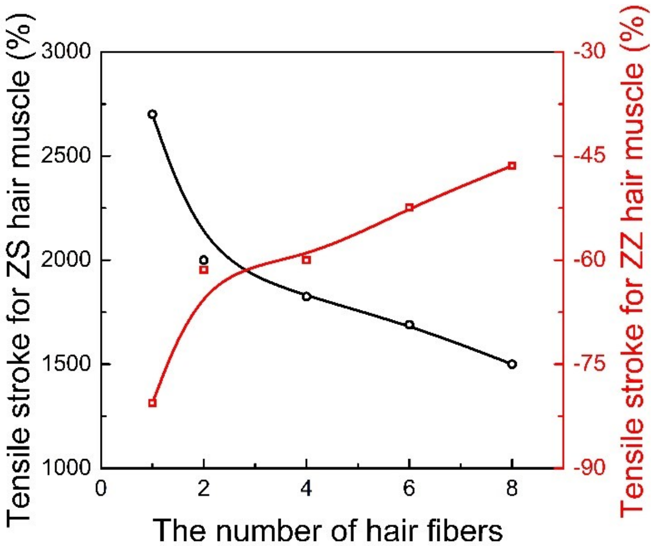

Figure S23. Tensile stroke for the homochiral and the heterochiral hair coils with different number of plies of the hair fibers on exposure to the water fog. The hair coil was soaked in the ammonium thioglycollate solution (600 mM) for 15 min for reduction, followed by soaking in the lauramine oxide solution (130 mM) for 10 min for oxidation; the twist density was 2000 turns m^{-1}, the spring index was 15.8, the coil pitch for the homochiral coil was 3 mm and the coils contacted each other for the heterochiral coils, and the flux of the water fog was 0.22 g s^{-1} m^{-1}.

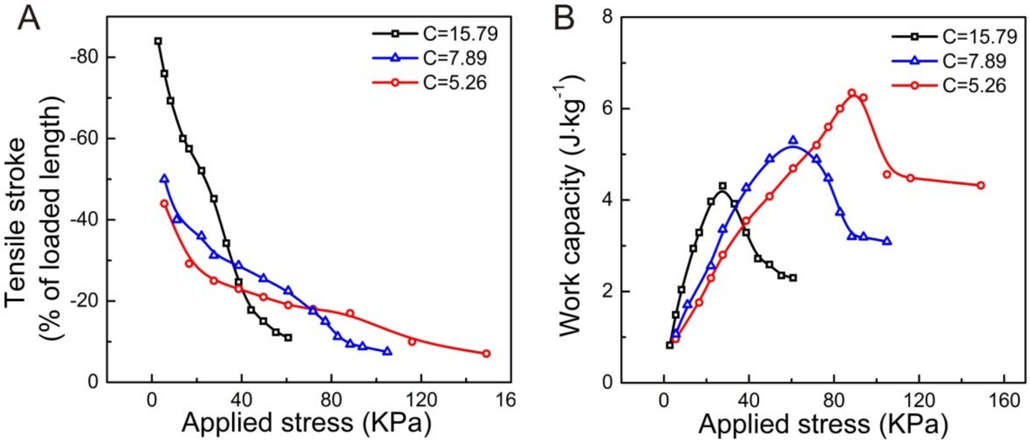

Figure S24c. (A) Tensile stroke and (B) the work capacity as a function of the applied stress for the homochiral hair coils with different spring index on exposure to the water fog. The hair coils were soaked in the ammonium thioglycollate solution (600 mM) for 15 min for reduction, followed by soaking in the lauramine oxide solution (130 mM) for 10 min for oxidation; the twist density was 2000 turns m^{-1}, the coil pitch was 3 mm, and the flux of the water fog was 0.22 g s^{-1} m^{-1}.

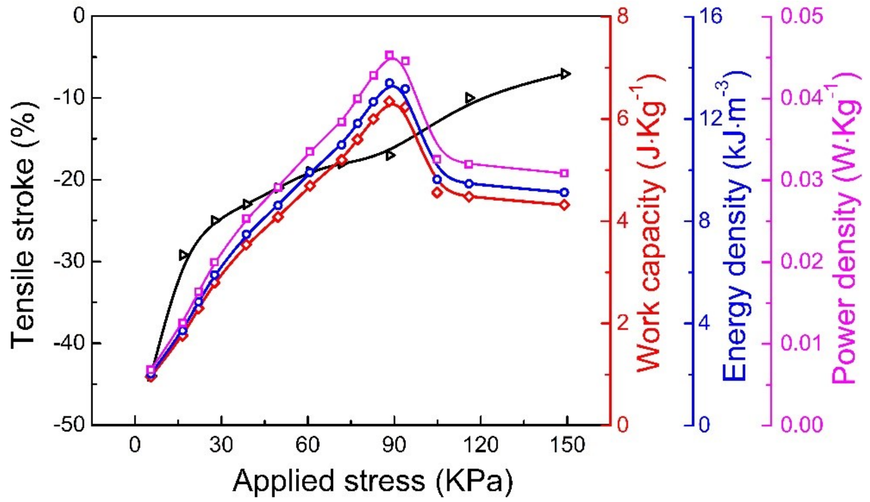

Figure S25. The tensile stroke, the work capacity, the energy density and the power density as a function of the applied stress for the homochiral hair coil on exposure to the water fog. The hair coil was soaked in the ammonium thioglycollate solution (600 mM) for 15 min for reduction, followed by soaking in the lauramine oxide solution (130 mM) for 10 min for oxidation; the twist density was 2000 turns m^{-1}, the spring index was 5.3, the coil pitch was 3 mm, and the flux of the water fog was 0.22 g s^{-1} m^{-1}.

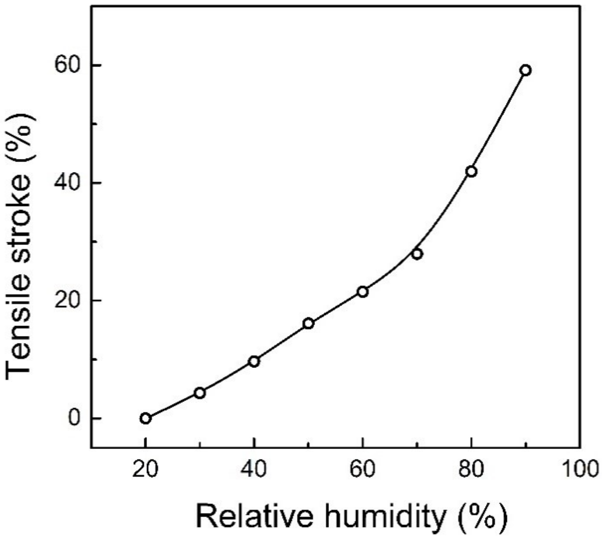

Figure S26. The tensile stroke as a function of the relative humidity for the moisture sensor fabricated by the homochiral hair coil. The coil were soaked in the ammonium thioglycollate solution (600 mM) for 15 min for chemical reduction, followed by soaking in the lauramine oxide solution (130 mM) for 10 min for chemical oxidation. The spring index was 2.8, the coil pitch was 3 mm, the twist density was 1000 turns m^{-1}, and the ambient humidity was ~20%.

3. Supplementary Tables

Table S1. Comparison of the torsional actuation properties of the hygromorph torsional fiber muscles, which were experimentally measured in this work.

Fiber materials	Twist density (turns mm^{-1})	Diameter (μm)	Rotation angle (° mm^{-1})	Rotation angle × Diameter (°)
Human hair	2.5	95	136	12.9
Silkworm silk	2.5	19	247	4.7
Cotton	2.5	16.6	199	3.3
CNT yarn	2.5	40	61.3	2.5
Wool	2.5	60	149	8.9

Table S2. Comparison of the tensile actuation stroke and the response rate of the hygromorph tensile artificial muscles in this work with literature results.

Fiber materials	Reversible or irreversible	Maximum contractile stroke (%)	Response rate (% s^{-1})
Human hair (This work)	Both	94	0.63
Graphene oxide fiber[3]	Reversible	5	0.5
CNT/silk fiber[4]	Reversible	0.4	0.0017
Silkworm[2]	Reversible	70	1.04
NT/hydrogel muscle[5]	Reversible	78	0.072
Spider silk[6]	Reversible	0.5	0.025

4. Movie Captions:

Movie S1. A hygrometer indicating changes in the ambient humidity.

A homochiral hair muscle can be directly used as an optically readable moisture sensor because it exhibited monotonically decreased length when equilibrated in different-humidity environment. For the preparation of the homochiral coil, ten plies of the hair fibers were twisted and folded in the middle, then wrapped around a mandrel to form a homochiral coil, next soaked in the ammonium thioglycollate solution (600 mM) for 15 min for chemical reduction, followed by soaking in the lauramine oxide solution (130 mM) for 10 min for chemical oxidation. The spring index was 13.89, the coil pitch was 3 mm, and the twist density was 1000 turns m^{-1}.

Movie S2. A moisture-sensitive electrical switch made of the homochiral hair muscle.

A homochiral hair coil was used as a hygromorph electrical switch for a smart alarm. In the dry air (20%), the light emitting diodes (LEDs) were connected to the electrical supply by the copper plate connected to the end of the hair coil muscle and lightened; when the hair coil was exposed to the water fog, the electric circuit was disconnected, and the LEDs went out.

For the preparation of the homochiral coil, ten plies of the twisted hair fibers were fold in the middle, then wrapped around a mandrel to form a homochiral coil, and they were soaked in the ammonium thioglycollate solution (600 mM) for 15 min for chemical reduction, followed by soaking in the lauramine oxide solution (130 mM) for 10 min for chemical oxidation. The spring index was 2.78, the coil pitch was 3 mm, the twist density was 1000 turns m^{-1}, and the ambient humidity was ~20%.

Movie S3. Crawling soft robot like caterpillar.

Two individually parallel aligned coiled heterochiral hair muscles with reversible actuation were used for preparing a water fog-controlled crawling soft robot. Two heterochiral coil hair muscles were parallelly assembled on three feet with single orientation to make a crawling robot. The soft crawling robot can crawl forward on a flat surface by applying/removing the water fog.

Movie S4. A smart hair style that getting short upon exposure to the water droplets and recovering the shape upon drying.

To prepare the hair coils, ten plies of the twisted hair fibers were wrapped around a mandrel to form a homochiral coil, and then they were soaked in the ammonium thioglycollate solution (600 mM) for 15 min for chemical reduction, followed by soaking in the lauramine oxide solution (130 mM) for 10 min for chemical oxidation. The as-prepared hair coils showed reversible hydromorphic actuation. The spring index was 15.8, the coil pitch was 3 mm, the twist density was 2000 turns m^{-1}, and the ambient humidity was 20%.

Movie S5. Comparison of the torsional free reversible tensile artificial muscles made by the hair and the silkworm silk when exposing to hot water fog.

The twisted hair fiber was folded in the middle, then heterchirally wrapped around a mandrel to form a homochiral coil, next soaked in the ammonium thioglycollate solution (600 mM) for 15 min for chemical reduction, followed by soaking in the lauramine oxide solution (130 mM) for 10 min for chemical oxidation. Twisted silkworm fiber was wrapped around a mandrel to form a heterochiral coil, and then it was thermally annealed at 120 ℃ for 30 min. The spring index was 13.89, the coil pitch was 3 mm, and the twist density was 1000 turns m^{-1}.

5. Supplementary References:

(1) C. S. Haines, M. D. Lima, N. Li, G. M. Spinks, J. Foroughi, J. D. Madden, S. H. Kim, S. Fang, M. J. Andrade, F. Göktepe and et al. Science 2014, 343(6173), 868-872.

(2) T. Jia, Y. Wang, Y. Dou, Y. Li, M. Jung de Andrade, R. Wang, S. Fang, J. Li, Z. Yu R. Qiao and et al. *Adv. Funct. Mater.* 2019, 29(18), 1808241.

(3) H. Cheng, J. Liu, Y. Zhao, C. Hu, Z. Zhang, N. Chen, L. Jiang and L. Qu, *Angew. Chem. Int. Edit.* 2013, 52(40), 10482-10486.

(4) E. Steven, W. R. Saleh, V. Lebedev, S. F. Acquah, V. Laukhin, R. G. Alamo and J. S. Brooks, *Nat. Commun.* 2013, 4, 2435.

(5) S. H. Kim, C. H. Kwon, K. Park, T. J. Mun, X. Lepró, R. H. Baughman, G. M. Spinks and S. J. Kim, *Sci. Rep.* 2016, 6, 23016.

(6) I. Agnarsson, A. Dhinojwala, V. Sahni and T. A. Blackledge, *J. Exp. Biol.* 2009, 212(13), 1990-1994.